Supporting Information

Nonadditive ion effects on the coil-globule equilibrium of PNIPAM: A computer simulation study

Yani Zhao[†], Swaminath Bharadwaj[†], and Nico F. A. van der Vegt

Contents

Eduard-Zintl-Institut für Anorganische und Physikalische Chemie, Technische Universität Darmstadt, Alarich-Weiss-Strasse 10, 64287 Darmstadt, Germany
*E-mail: zhao@cpc.tu-darmstadt.de; bharadwaj@cpc.tu-darmstadt.de; vandervegt@cpc.tu-darmstadt.de
† These authors contributed equally

S1 Coil-globule equilibrium

The LCST-type transition in aqueous solutions of PNIPAM is experimentally observed to be first order (two state).[1–3] Such a two state behaviour has also been observed in the coil-to-globule transitions of short polymer chains in simulation studies.[4,5] Therefore, the experimental salting in/out behaviour of PNIPAM will herein be correlated with salt effects on the single-chain coil-globule equilibrium. To probe the salt effects on the coil and globule states, the simulation trajectories were separated into coil and globule structural ensembles using the radius of gyration, R_g, as a criterion for distinguishing between coils and globules.[6–8] As in the work of Dalgicdir et al.,[7] a configuration was considered to be part of the ensemble of coil structures for $R_g > 1.8$ nm, and was considered to be part of the ensemble of globule structures for $R_g < 1.2$ nm (see Fig. S1).

S2 Preferential binding coefficients

In this work, the preferential binding coefficients were computed using the following expression,[9]

$$\Gamma_{pa}(r) = \left\langle n_a(r) - \frac{N_a - n_a(r)}{N_w - n_w(r)} n_w(r) \right\rangle, \tag{S1}$$

where $n_a(r)$ and $n_w(r)$ are the number of ions (cations and anions considered indistinguishable) and the number of water molecules within a proximal distance of r from the polymer surface, respectively. N_a and N_w are the total number of ions and water molecules in the system, respectively. Similarly, one can also define preferential binding coefficients for different ions such as iodide and sulfate in the following way,

$$\begin{aligned} \Gamma_{pI}(r) &= \left\langle n_I(r) - \frac{N_I - n_I(r)}{N_w - n_w(r)} n_w(r) \right\rangle, \\ \Gamma_{pS}(r) &= \left\langle n_S(r) - \frac{N_S - n_S(r)}{N_w - n_w(r)} n_w(r) \right\rangle, \end{aligned} \tag{S2}$$

where $n_I(r)$ and $n_S(r)$ are the number of iodide and sulfate ions within a proximal distance of r from the polymer surface, respectively. N_I and N_S are the total number of iodide and sulfate ions in the system, respectively.

S2.1 Pure NaI solutions

Figures S2a and S2b show the dependence of the preferential binding coefficients, $\Gamma^C_{pa}(r), \Gamma^G_{pa}(r)$, on the proximal distance, r, from the polymer at different c_{NaI} in the absence of the background salt. The thermodynamic limiting values of the preferential binding coefficients were evaluated by averaging in the range 0.8 nm < r < 1.2 nm. Ions are depleted from both the coil and globule states at all NaI concentrations. At low (high) concentrations, ions deplete to a larger extent from the globule (coil) state thereby shifting the coil-globule equilibrium towards the coil (globule) state. Figures S3a and S3b show the dependence of the preferential binding coefficients, $\Gamma^C_{pI}(r), \Gamma^G_{pI}(r)$, on the proximal distance, r, from the polymer at different c_{NaI} in the absence of the background salt. The thermodynamic limiting values of the preferential binding coefficients were evaluated by averaging in the range 0.8 nm < r < 1.2 nm. Here, it can be seen that the trends in the depletion of iodide ions from the coil and globule states are similar to the trends in Fig. S2.

S2.2 Mixed salt solutions

Figure S4a shows the dependence of the preferential binding coefficients, $\Gamma^C_{pa}(r), \Gamma^G_{pa}(r)$, on the proximal distance, r, from the polymer at different c_{NaI} in the presence of the background salt. Ions are depleted from both the coil and globule states at all NaI concentrations. In contrast to pure NaI solutions, ions are always depleted to a larger extent from the coil state, at low NaI concentrations (region I), thereby shifting the coil-globule equilibrium to the globule state. Note, from Fig. S4b, that the preferential binding coefficients for the sulfate ions, $\Gamma^C_{pS}(r), \Gamma^C_{pS}(r)$, show a similar dependence on c_{NaI} at low NaI concentrations. On the other hand, from Figs. S5a and S5b, it can be seen the iodide ions are preferentially adsorbed on both the coil and globule states and shift the coil-globule equilibrium towards the coil state.

The thermodynamic limiting values of the preferential binding coefficients, for the mixed salt solutions, were evaluated by averaging in the range, 1.8 nm < r < 2.5 nm, for $c_{NaI} = 0.05$ m and in the range, 1.5 nm < r < 2.0 nm, for other concentrations.

S3 Ion pairing and ion hydration

The excess ion pairing (or affinity), $\Delta N_{an,cat}$, between an anion (an) and a cation (cat) is defined as

$$\Delta N_{an,cat} = \frac{N_{cat}}{V} \int_{r_{in}}^{r_{out}} [g_{an,cat}(r) - 1] 4\pi r^2 dr \tag{S3}$$

where $g_{an,cat}$ is the anion-cation radial distribution function, V is the average volume of the simulation box and N_{cat} the total number of cations. $\Delta N_{an,cat}$ can be interpreted as the change in the number of cations in a spherical observation region before and after placing

Table S1 Radii r_{in} and r_{out} used for the calculation of excess anion-cation contact ion pairing (CIP), solvent shared ion pairing (SIP) and solvent separated ion pairing (SSIP). Radii r_{in} and r_{out} used for the calculation of excess hydration (water affinity) of the 1st and 2nd hydration shells of the iodide and sulfate ions.

		CIP		SIP		SSIP	
		r_{in}	r_{out}	r_{in}	r_{out}	r_{in}	r_{out}
I^-	Na^+	0	0.41 nm	0.41 nm	0.65 nm	-	-
SO_4^{2-}	Na^+	-	-	0	0.68 nm	0.68 nm	0.92 nm
		1st hydration shell		2nd hydration shell			
I^-	OW ($c_{Na_2SO_4} = 0$ m)	0	0.42 nm	0.42 nm	0.66 nm		
I^-	OW ($c_{Na_2SO_4} = 0.3$ m)	0	0.42 nm	0.42 nm	0.64 nm		
SO_4^{2-}	OW	0	0.44 nm	0.44 nm	0.68 nm		

an anion at the center of this region. r_{in} and r_{out} enable us to calculate the excess CIP, excess SIP, excess SSIP or a combination of them (see vertical dotted lines in Figs. S6a, S6b and S9a). Table S1 summarises the values of r_{in} and r_{out} for CIP, SIP and SSIP for different cation-anion combinations. A similar expression can be defined for the anion-water affinity in the following manner

$$\Delta N_{an,w} = \frac{N_w}{V} \int_{r_{in}}^{r_{out}} [g_{an,w}(r) - 1] 4\pi r^2 dr \tag{S4}$$

where $g_{an,w}$ is the anion-water radial distribution function and N_w the total number of water molecules. $\Delta N_{an,w}$ is the anion-water affinity and can be defined as the change in the number of water molecules in a spherical observation region before and after placing an anion at the center of this region. Table S1 summarises the values of r_{in} and r_{out} for the 1st and 2nd hydration shell of different anions. The different rdfs were calculated using the subroutine "rdf" in GROMACS.[10] The finite size effects in the rdfs were corrected using the Ganguly correction.[11]

$$g_{ij}^{corrected}(r) = g_{ij}(r) \frac{N_j \left(1 - \frac{(4/3)\pi r^3}{V}\right)}{N_j \left(1 - \frac{(4/3)\pi r^3}{V}\right) - \Delta N_{ij}(r) - \delta_{ij}} \tag{S5}$$

where N_j is the number of particles of type j in the system, V is the system volume and $\Delta N_{ij}(r)$ is the excess number of particles of type j within a sphere of radius r around particle i. On this rdf correction, the extrapolated KBI correction proposed by Krüger et al. was applied.[12]

$$G_{ij}(R) = \int_0^R \omega(r,R)(g_{ij}^{corrected}(r) - 1) dr \tag{S6}$$

where

$$\omega(r,R) = 4\pi r^2 \left[1 - \left(\frac{r}{R}\right)^3\right] \tag{S7}$$

This combination of the KBI and rdf corrections has been shown to yield improved KBI convergence in ideal and nonideal aqueous mixtures.[13]

S3.1 Iodide-sodium affinity

Figures S6a and S6b show the iodide-sodium radial distribution functions (rdf) at different NaI concentrations in the presence and absence of the background salt, $c_{Na_2SO_4} = 0.3$ m. The first and second peaks in the iodide-sodium rdf correspond to contact ion pairing and solvent shared ion pairing. Figures S6c and S6d show that the excess contact ion pairing and the excess solvent shared ion pairing, respectively. From Fig. 6a in the main text, it can be seen that the excess iodide-sodium ion pairing in mixed salt solutions is smaller as compared to pure NaI solutions at all NaI concentrations. This can be attributed to the iodide-sodium excess contact ion pairing in mixed salt solutions which decreases with the concentration of NaI but is smaller as compared to pure NaI solutions (see Fig. S6c).

S3.2 Iodide-water affinity

Figures S7a and S7b show the iodide-water rdfs at different NaI concentrations in the presence and absence of the background salt, $c_{Na_2SO_4} = 0.3$ m. The first and second peaks in the iodide-water rdf correspond to first and second hydration shell, respectively. Figures S7c and S7d show that the iodide-water affinity in the first and second hydration shell respectively. From Fig. S7c, it can be seen that the first hydration shell of the iodide ions is not perturbed significantly by the background salt.

S3.3 Sulfate-water affinity

Figure S8a shows the sulfate-sodium rdf at different NaI concentrations ($c_{Na_2SO_4} = 0.3$ m). The first and second peaks in the sulfate-water rdf correspond to first and second hydration shell, respectively. Figures S8b and S8c show that trends in the excess solvent shared

Table S2 Comparison of $\Delta T(c_{\mathrm{NaI}})$ obtain from simulation with $\Delta\mathrm{LCST}(c_{\mathrm{NaI}})$ from experimental meaurements, for pure NaI and mixed salt solutions. The experimental data was adopted from ref.[16]

$c_{\mathrm{Na_2SO_4}}$ $[m]$	c_{NaI} [m]	$\Delta\Gamma_{\mathrm{pa}}^{\mathrm{C}\to\mathrm{G}}$ (pure NaI)	$\Delta T = T_{\mathrm{c}} - T_{\mathrm{c}}(c_{\mathrm{NaI}}=0)$ (sim)°C	ΔLCST(exp) °C
0	0.05	-0.099082	0.36342	0.269
0	0.1	-0.00595	0.021842	0.373
0.3	0.05	3.9929	-1.489	-2.42
0.3	0.1	4.1289	-2.220	-2.73

ion pairing and the excess solvent separated ion pairing, respectively.

S3.4 Sulfate-sodium affinity

Figure S9a shows the sulfate-sodium rdf at different NaI concentrations ($c_{\mathrm{Na_2SO_4}} = 0.3$ m). The first and second peaks in the iodide-sodium rdf correspond to solvent shared ion pairing and solvent separated ion pairing. Note that sulfate and sodium ions do not form contact ions pairs. Figures S9b and S9c show that the trends in the excess solvent shared ion pairing and the excess solvent separated ion pairing, respectively.

S4 Relation between the preferential binding coefficients and the change in LCST

We used the semi-quantitative theoretical framework proposed by Heyda and Dzubiella to relate the preferential binding coefficients of the coil and globule states, $\Gamma_{\mathrm{pa}}^{\mathrm{C}}$ and $\Gamma_{\mathrm{pa}}^{\mathrm{G}}$, to the change in the LCST, ΔLCST, with increase in the ion concentration.[14] The two-state coil-globule equilibrium in aqueous ion solutions is determined by the polymer collapse free energy, $\Delta G^{\mathrm{C}\to\mathrm{G}} = \Delta G^{\mathrm{G}} - \Delta G^{\mathrm{C}}$, which depends on the salt concentration and temperature. For small changes in salt concentration and temperature, $\Delta G^{\mathrm{C}\to\mathrm{G}}(c,T)$ can be Taylor-expanded (upto to the first order term) with respect to the variables c and T, taking the neat water state $(c=0)$ at T_0 as the reference state,

$$\Delta G^{\mathrm{C}\to\mathrm{G}}(c, T = T_0 + \Delta T) \approx \Delta G^{\mathrm{C}\to\mathrm{G}}(0,T_0) + \left(\frac{\partial \Delta G^{\mathrm{C}\to\mathrm{G}}}{\partial T}\right)_{0,T_0} \Delta T + \left(\frac{\partial \Delta G^{\mathrm{C}\to\mathrm{G}}}{\partial c}\right)_{0,T_0} \Delta c \tag{S8}$$

where $\Delta G^{\mathrm{C}\to\mathrm{G}}(0,T_0)$ is the polymer collapse free energy in neat water solutions at temperature T_0. The above equation assumes that the polymer collapse free energy, $\Delta G^{\mathrm{C}\to\mathrm{G}}(c,T)$, has a linear dependence on the salt concentration and temperature. For a given salt concentration c, $\Delta G^{\mathrm{C}\to\mathrm{G}}(c, T_{\mathrm{c}}(c))$ is zero at the transition temperature T_{c}. If $\Delta T = T_{\mathrm{c}}(c) - T_{\mathrm{c}}(c=0)$, then the above equation can be rewritten in the following way,

$$\left(\frac{\partial \Delta G^{\mathrm{C}\to\mathrm{G}}}{\partial T}\right)_{0,T_c(c=0)} \Delta T \simeq -\left(\frac{\partial \Delta G^{\mathrm{C}\to\mathrm{G}}}{\partial c}\right)_{0,T_c(c=0)} \Delta c, \tag{S9}$$

Note that, for aqueous PNIPAM solutions, the LCST and coil-to-globule transition temperature, T_{c}, are equal.[15] Combining the above expression with $\left(\partial \Delta G^{\mathrm{C}\to\mathrm{G}}/\partial c_{\mathrm{a}}\right)_{p,T} = -RT\Delta\Gamma_{\mathrm{pa}}^{\mathrm{C}\to\mathrm{G}}/(c_{\mathrm{a}}\,(1 + c_{\mathrm{a}}\,(G_{\mathrm{aa}} - G_{\mathrm{aw}}))$ and assuming that the factor, $1 + c_{\mathrm{a}}(G_{\mathrm{aa}} - G_{\mathrm{aw}}) \approx 1$, we obtain

$$\Delta T \simeq -\frac{RT\Delta\Gamma_{\mathrm{pa}}^{\mathrm{C}\to\mathrm{G}}}{\Delta S_0^{\mathrm{C}\to\mathrm{G}}}, \tag{S10}$$

where $\Delta S_0^{\mathrm{C}\to\mathrm{G}} = -\left(\partial \Delta G^{\mathrm{C}\to\mathrm{G}}/\partial T\right)_{0,T_c(c=0)}$ is the polymer collapse entropy in neat water solutions. $\Delta S_0^{\mathrm{C}\to\mathrm{G}}$ has been measured by different techniques and has a median value of is 17 J mol^{-1}K^{-1} per monomer.[14] Therefore, for a 40mer chain, $\Delta S_0^{\mathrm{C}\to\mathrm{G}} = 0.68$ kJ mol^{-1}K^{-1}. The $\Delta\Gamma_{\mathrm{pa}}^{\mathrm{C}\to\mathrm{G}}$ values from the pure NaI and mixed salt solutions (Fig. 1b and 1d) were employed to calculate $\Delta T(c_{\mathrm{NaI}})$ which were subsequently compared with the experimental data for $\Delta\mathrm{LCST}(c_{\mathrm{NaI}})$ (see Table S2). From Table S2, it can be seen that, apart from the case of $c_{\mathrm{NaI}} = 0.1$ m, $\Delta T(c_{\mathrm{NaI}})$ from the simulations is in agreement with the experimentally measured $\Delta\mathrm{LCST}(c_{\mathrm{NaI}})$. Note that $\Delta G^{\mathrm{C}\to\mathrm{G}}$ has a non-monotonic dependence on the NaI concentration in pure NaI concentrations where it first increases with increase in NaI and subsequently decreases with increase in NaI. The transition between the regimes occurs at $c_{\mathrm{NaI}} \approx 100$ mM where the assumption of linear dependence of $\Delta G^{\mathrm{C}\to\mathrm{G}}$ is no longer valid. This is the reason for the large mismatch between the experimental and simulation ΔT.

References

1 C. Wu and X. Wang, *Phys. Rev. Lett.*, 1998, **80**, 4092–4094.
2 X. Wang, X. Qiu and C. Wu, *Macromolecules*, 1998, **31**, 2972–2976.
3 E. I. Tiktopulo, V. N. Uversky, V. B. Lushchik, S. I. Klenin, V. E. Bychkova and O. B. Ptitsyn, *Macromolecules*, 1995, **28**, 7519–7524.
4 V. Palivec, D. Zadrazil and J. Heyda, 2018, arXiv:1806.05592.
5 M. Podewitz, Y. Wang, P. K. Quoika, J. R. Loeffler, M. Schauperl and K. R. Liedl, *J. Phys. Chem. B*, 2019, **123**, 8838–8847.
6 C. Dalgicdir, F. Rodríguez-Ropero and N. F. A. van der Vegt, *J. Phys. Chem. B*, 2017, **121**, 7741–7748.
7 C. Dalgicdir and N. F. A. van der Vegt, *J. Phys. Chem. B*, 2019, **123**, 3875–3883.
8 D. Nayar, A. Folberth and N. F. A. van der Vegt, *Phys. Chem. Chem. Phys.*, 2017, **19**, 18156–18161.
9 V. Pierce, M. Kang, M. Aburi, S. Weerasinghe and P. E. Smith, *Cell Biochem. Biophys.*, 2008, **50**, 1–22.
10 M. J. Abraham, T. Murtola, R. Schulz, S. Páll, J. C. Smith, B. Hess and E. Lindahl, *SoftwareX*, 2015, **1**, 19–25.
11 P. Ganguly and N. F. A. van der Vegt, *J. Chem. Theory Comput.*, 2013, **9**, 1347–1355.
12 P. Krüger, S. K. Schnell, D. Bedeaux, S. Kjelstrup, T. J. H. Vlugt and J.-M. Simon, *J. Phys. Chem. Lett.*, 2013, **4**, 235–238.
13 J. Milzetti, D. Nayar and N. F. A. van der Vegt, *J. Phys. Chem. B*, 2018, **122**, 5515–5526.
14 J. Heyda and J. Dzubiella, *J. Phys. Chem. B*, 2014, **118**, 10979–10988.
15 I. Bischofberger, D. C. E. Calzolari and V. Trappe, *Soft Matter*, 2014, **10**, 8288–8295.
16 E. E. Bruce, P. T. Bui, B. A. Rogers, P. S. Cremer and N. F. A. van der Vegt, *J. Am. Chem. Soc.*, 2019, **141**, 6609–6616.

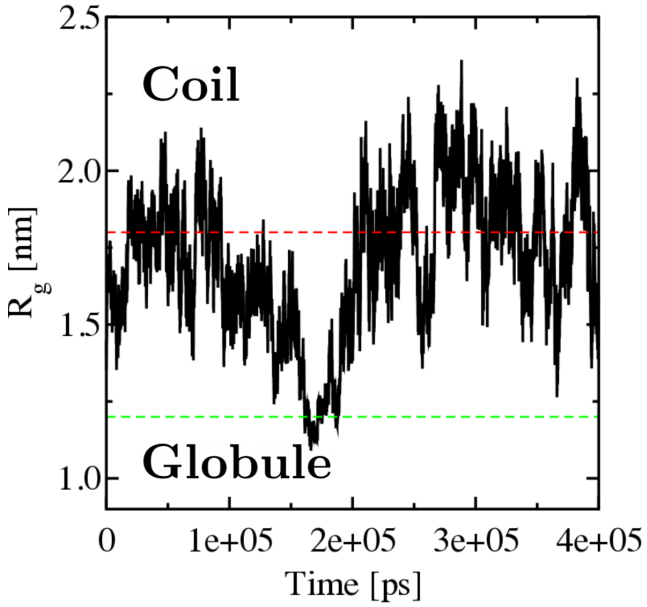

Fig. S1 Dependence of the radius of gyration, R_g, on the simulation time in PNIPAM solutions with $c_{NaI} = 0.05$ m and $c_{Na_2SO_4} = 0.3$ m at 300 K. Configurations above $R_g > 1.8$ nm (red dashed line) are considered to be part of the coil ensemble. Configurations below the green dashed lines ($R_g < 1.2$ nm) are considered to part of the globule ensemble.

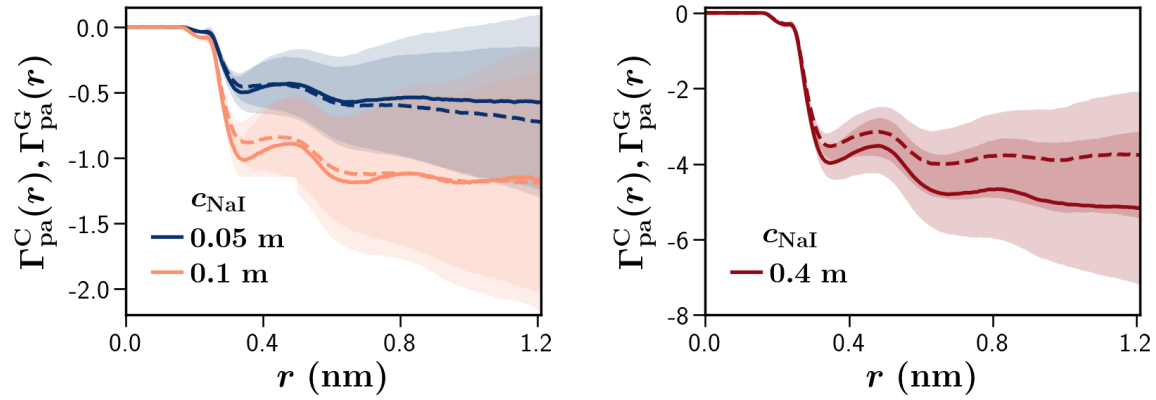

Fig. S2 All ions: dependence of the preferential binding coefficients of the coil, Γ^C_{pa} (solid lines), and globule, Γ^G_{pa} (dashed lines), states on the proximal distance r from the polymer surface at (a) c_{NaI}=0.05 m, 0.1 m and (b) c_{NaI}=0.4 m. In these cases, $c_{Na_2SO_4} = 0$. The shaded intervals indicate the standard deviation of the mean, $\sigma/\sqrt{N}$, using sample standard deviations, σ, and $N = 10$ blocks, respectively.

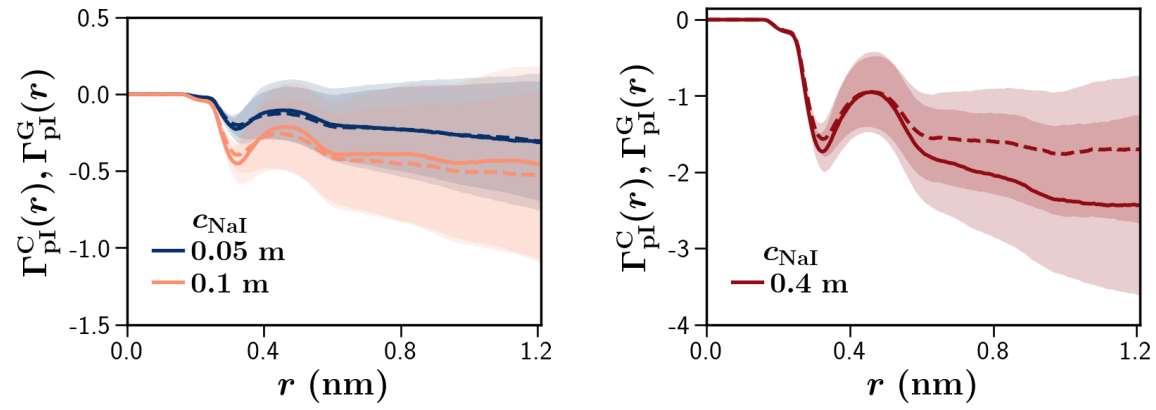

(a) (b)

Fig. S3 Iodide ions: dependence of the preferential binding coefficients of the coil, Γ^{C}_{pI} (solid lines), and globule, Γ^{G}_{pI} (dashed lines), states on the proximal distance r from the polymer surface at (a) c_{NaI}=0.05 m, 0.1 m and (b) c_{NaI}=0.4 m. In these cases, $c_{Na_2SO_4} = 0$. The shaded intervals indicate the standard deviation of the mean, $\sigma/\sqrt{N}$, using sample standard deviations, σ, and $N = 10$ blocks, respectively.

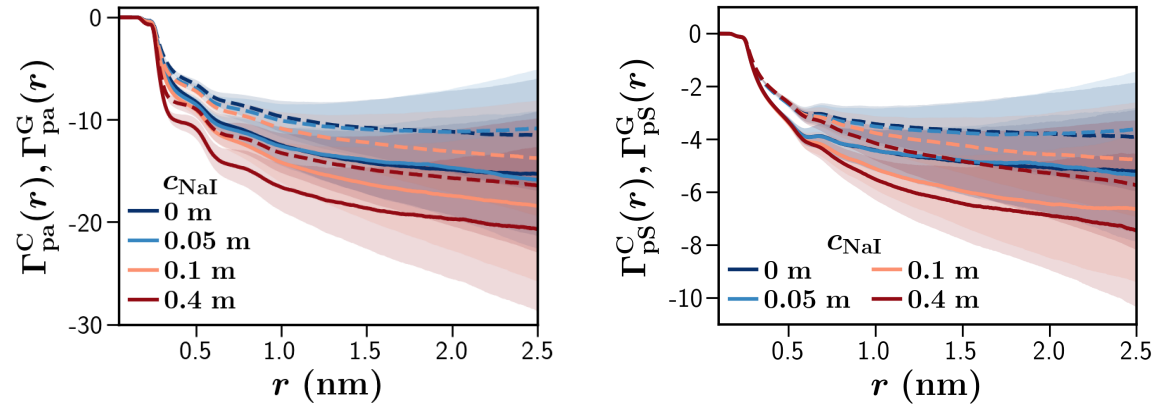

(a) (b)

Fig. S4 Dependence of the preferential binding coefficients of the coil (solid lines) and globule (dashed lines) states on the proximal distance r from the polymer surface at different NaI concentration for (a) all ions (Γ^{C}_{pa}, Γ^{G}_{pa}) and (b) sulfate ions (Γ^{C}_{pS}, Γ^{G}_{pS}). In these cases, the concentration of the background salt is fixed at $c_{Na_2SO_4} = 0.3$ m. The shaded intervals indicate the standard deviation of the mean, $\sigma/\sqrt{N}$, using sample standard deviations, σ, and $N = 10$ blocks, respectively.

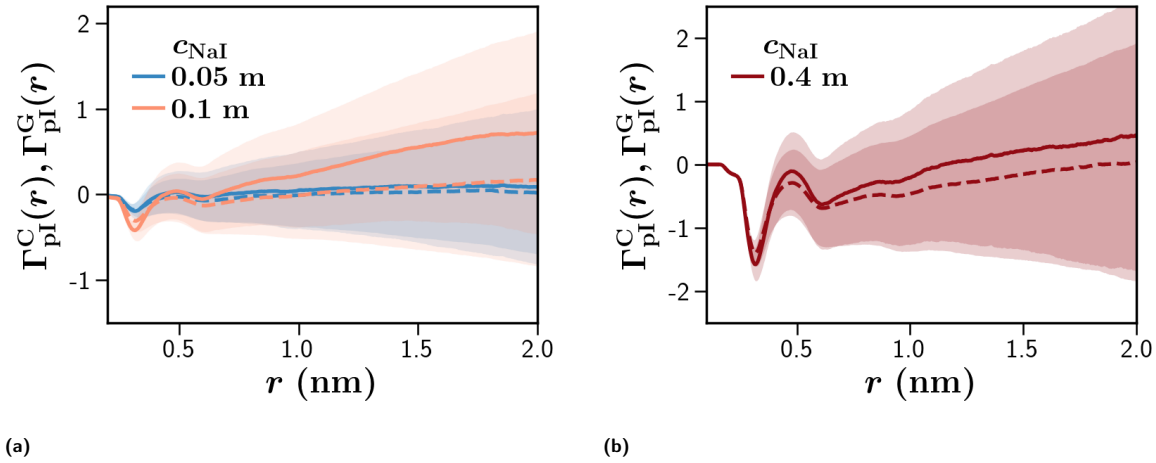

Fig. S5 Iodide ions: dependence of the preferential binding coefficients of the coil, $\Gamma^{\mathrm{C}}_{\mathrm{pI}}$ (solid lines), and globule, $\Gamma^{\mathrm{G}}_{\mathrm{pI}}$ (dashed lines), states on the proximal distance r from the polymer surface at (a) c_{NaI}=0.05 m, 0.1 m and (b) c_{NaI}=0.4 m. In these cases, the concentration of the background salt is fixed at $c_{\mathrm{Na_2SO_4}} = 0.3$ m. The shaded intervals indicate the standard deviation of the mean, $\sigma/\sqrt{N}$, using sample standard deviations, σ, and $N = 10$ blocks, respectively.

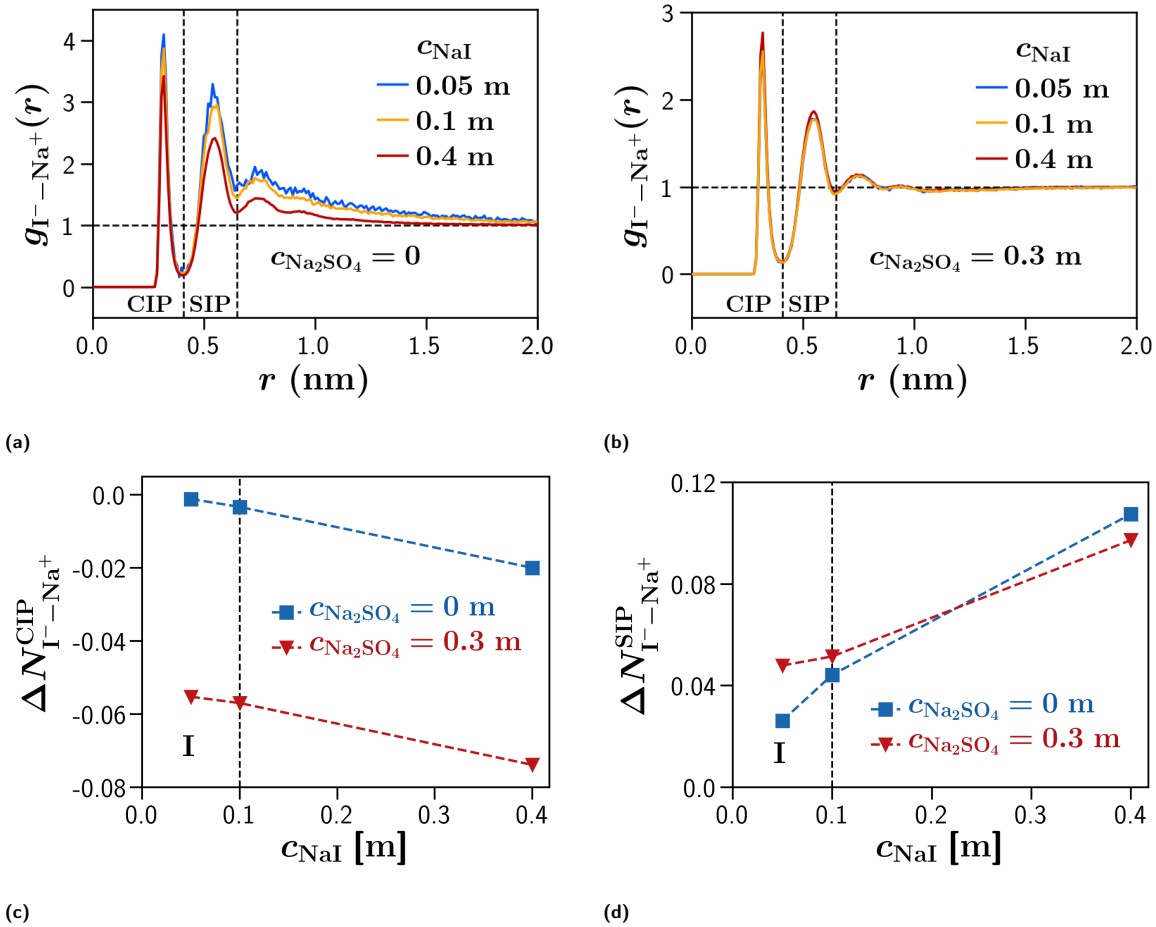

Fig. S6 Iodide-sodium: dependence of the iodide-sodium radial distribution function, $g_{\mathrm{I^-\!-\!Na^+}}$, on the distance r for different c_{NaI} at (a) $c_{\mathrm{Na_2SO4}} = 0$ and (b) $c_{\mathrm{Na_2SO4}} = 0.3$ m. Dependence of the excess ion pairing between iodide and sodium on c_{NaI}, in the presence and absence of sodium sulfate, for (c) contact ion pairs (CIP) and (d) solvent shared ion pairs (SIP). The vertical lines in (a) and (b) indicate the regions from which the excess ion pairing is calculated for CIP and SIP.

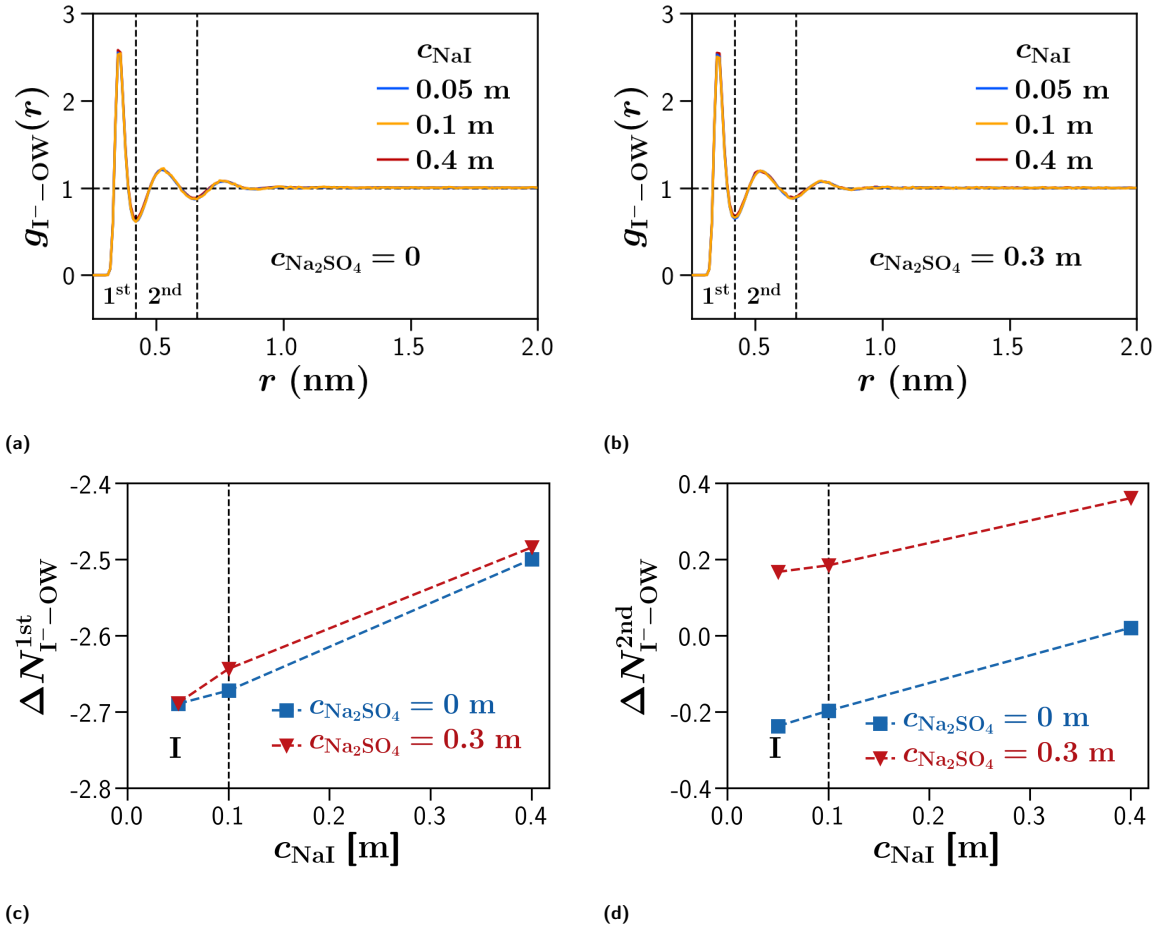

Fig. S7 Iodide-water: dependence of the iodide-water radial distribution function, $g_{\mathrm{I^-\!-\!OW}}$, on the distance r for different c_{NaI} at (a) $c_{\mathrm{Na_2SO4}} = 0$ and (b) $c_{\mathrm{Na_2SO4}} = 0.3$ m. Dependence of the iodide-water affinity on c_{NaI}, in the presence and absence of sodium sulfate, for (c) the 1st hydration shell (d) 2nd hydration shell. The vertical lines in (a) and (b) indicate the regions from which the iodide-water affinity is calculated for the 1st and 2nd hydration shells.

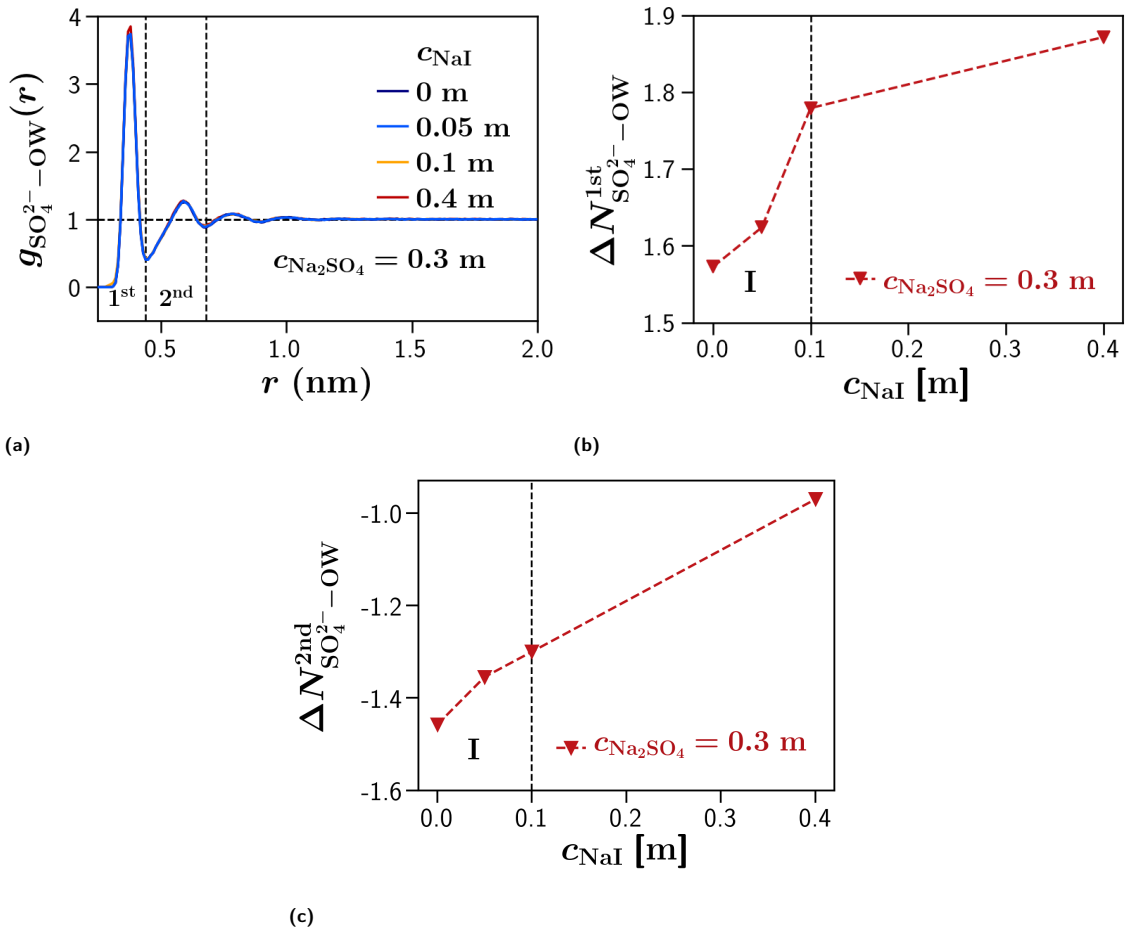

Fig. S8 Sulfate-water: (a) dependence of the sulfate-water radial distribution function, $g_{\mathrm{SO_4^{2-}-OW}}$, on the distance r for different c_{NaI} at $c_{\mathrm{Na_2SO4}} = 0.3$ m. Dependence of the sulfate-water affinity on c_{NaI}, in the presence and absence of sodium sulfate, for (b) the 1st hydration shell (c) 2nd hydration shell. The vertical lines in (a) indicate the regions from which the iodide-water affinity is calculated for the 1st and 2nd hydration shells.

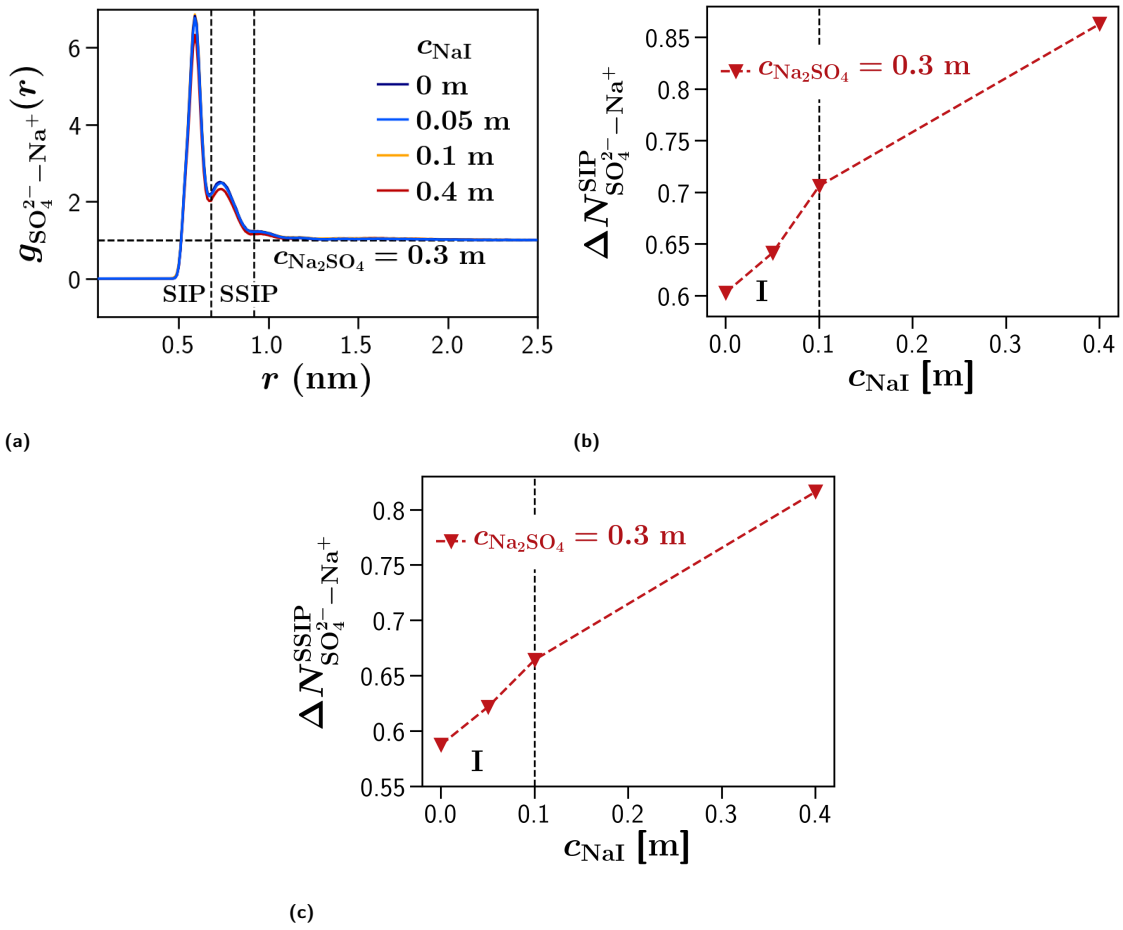

Fig. S9 Sulfate-sodium: (a) dependence of the sulfate-sodium radial distribution function, $g_{\mathrm{SO_4^{2-}-Na^+}}$, on the distance r for different c_{NaI} at $c_{\mathrm{Na_2SO4}} = 0.3$ m. Dependence of the excess ion pairing between sulfate and sodium on c_{NaI} for (b) solvent shared ion pairs (SIP) and (c) solvent separated ion pairs (SSIP). The vertical lines in (a) indicate the regions from which the excess ion pairing is calculated for SIP and SSIP.